PERGAMON

International Journal of Heat and Mass Transfer 41 (1998) 2847–2856

International Journal of HEAT and MASS TRANSFER

Radiative heat transfer in anisotropic scattering media with specular boundary subjected to collimated irradiation

Shigenao Maruyama*

Institute of Fluid Science, Tohoku University, Aoba-ku, Katahira 2-1-1, Sendai 980-77, Japan

Received 11 October 1996

Abstract

Generalized numerical method, radiation element method by ray emission model, REM^2, is applied to plane-parallel and anisotropic scattering participating media using the delta function approximation. The boundary can be specular and/or diffuse, and both collimated and diffuse incident irradiation can be specified on the boundary. REM^2 can be applied to various thermal conditions in the medium and boundaries. Good agreement is obtained between the present numerical solutions using the delta function approximation and existing exact solutions, even for strong forward and back scattering media. The proposed method is applied to an anisotropic scattering participating medium with a specular surface. The effect of specular reflectivity of scattering layers subjected to obliquely collimated flux was investigated.

Nomenclature

a_1 coefficient of Legendre polynomial $P_1(\mu)$, equations (8), (36)
A^R effective radiation area, equation (6)
$F^A_{i,j}$ absorption view factor, equation (19)
$F^D_{i,j}$ diffuse reflection view factor, equation (20)
$F^E_{i,j}$ extinction view factor, equation (17)
$I(x,\mu)$ radiation intensity
I_b blackbody radiation intensity
$I^D(x)$ diffuse radiation intensity
K number of discretized angles of ray emission
N total number of radiation elements
n refractive index
$P_n(\mu)$ Legendre polynomial of nth order
q_c collimated irradiation heat flux, σT_0^4, Fig. 1
q_X heat generation rate per unit volume or heat flux of boundary surface, equation (28)
$q^R(x)$ radiation flux at location x, equation (29)
$Q_{G,i}$ heat transfer rate of irradiation to element i, equation (21)
$Q_{J,i}$ diffuse radiation transfer rate from element i, equation (7)
$Q_{T,i}$ heat transfer rate of emissive power from element i, equation (22)
$Q_{X,i}$ net rate of heat transfer of element i, equation (23)
S path length of radiation
T temperature
T_0 reference temperature
w_k weight of discretized angle, Table 2
x location, Fig. 1
x_f thickness of participating medium, Fig. 1.

Greek symbols

β extinction coefficient of participating medium, $\kappa+\sigma_s$
β^* apparent extinction coefficient of anisotropic media, equation (15), Table 1
$\delta(1-\mu)$ dirac delta function
ΔE numerical deviation from exact solution %, equation (31)
Δx thickness of radiation element, Fig. 1
ε emissivity, $1-\Omega^D-\Omega^S$
θ polar angle, Fig. 1
θ_0 incident angle of collimated radiation flux, Fig. 1
κ absorption coefficient
λ wave length of radiation
μ direction cosine, $\cos\theta$
μ_k discretized angle, Table 2
ρ^R dimensionless reflected flux, equation (35)
σ Stefan–Boltzmann constant

* Corresponding author. Tel.: 0081 22 217 5243; fax: 0081 22 217 5243; e-mail: maruyama@ifs.tohoku.ac.jp.

0017-9310/98 $19.00
PII: S0017-9310(98)00055-6

σ_s scattering coefficient
τ^R dimensionless transmitted flux, equation (34)
τ_0 optical thickness of participating medium, βx_l
$\phi(\mu)$ phase function of scattering medium
Ψ dimensionless radiation flux, equation (30)
ω solid angle
Ω scattering albedo of participating medium, σ_s/β
Ω^D corrected diffuse scattering albedo or diffuse reflectivity, equation (16), Table 1
Ω^S specular reflectivity of boundary surface, Table 1.

Subscripts
1, N values on boundary surface, Fig. 1
exact exact solution
i, j values of element i and j, respectively
s value of boundary surface element
v value of volume element.

1. Introduction

Radiation transfer in participating media is important in the design of furnaces, precision heat-transfer control in semiconductor processes and prediction of the effect of dust, CO_2 and other participating gases on the global environment. Many methods have been developed to solve these problems, such as the Monte Carlo method by Siegel and Howell [1] and Yang et al. [2], the discrete ordinate method by Fiveland [3], the discrete transfer method by Lockwood and Shah [4], and the boundary element method by Bialecki [5]. However, it is difficult to apply these methods to complex three-dimensional configurations such as that used in finite element analysis.

The author [6] introduced a new definition of view factors and proposed a numerical method for analyzing three-dimensional (3-D) arbitrary surfaces with diffuse and specular reflections. Radiation transfer in a participating medium in a plane-parallel configuration was analyzed by Maruyama and Aihara [7] using the concept of view factors [6]. This concept was extended to the radiation element method by the ray emission model, REM^2 [8]. REM^2 is a generalized numerical method for analyzing radiation transfer in participating media and between specular and/or diffuse surfaces with arbitrary configurations and thermal conditions.

However, REM^2 can only be applied to isotropic scattering media, whereas most scattering particles are anisotropic scattering media [9]. Some numerical methods such as the discrete ordinate method and the P_N method take into account anisotropic scattering. When the discrete ordinate method is applied to a complex 3-D engineering model, the ray effect [10] is unavoidable unless a very large number of discrete ordinates are considered. Also these methods are very difficult to determine the radiative equilibrium temperature for a given heat transfer rate in the radiation element. The proposed method, REM^2, can easily be applied to the above mentioned complex systems. If REM^2 can be applied to anisotropic scattering media, then various engineering and environmental problems, with complex configurations and thermal conditions, can be analyzed.

Lee and Buckius [11] proposed an approximation that an anisotropic scattering medium is related to an isotropic one by scaling, and compared the radiation transfer in a plane-parallel system. The scaling was then extended to a two-dimensional (2-D) configuration [12]. Wiscombe [13] proposed the delta-M method in which the anisotropic phase function is approximated to low order Legendre polynomials. Crosbie and Davidson [14] proposed a similar approximation for the phase function using a delta function.

In the present study, REM^2 is applied to plane-parallel absorbing, emitting and scattering media with arbitrary thermal conditions in order to verify the applicability to anisotropic media. The surface boundary can be specular and/or diffuse with arbitrary thermal conditions. Diffuse or collimated irradiation can be applied at the boundary. The delta function approximation is used to scale the anisotropic scattering to isotropic scattering. The accuracy of the proposed method is confirmed by comparing with existing solutions for isotropic scattering media. The validity of the approximation for anisotropic scattering is verified by comparing the result obtained with existing exact solutions. Radiation transfer of an obliquely incident flux is analyzed, and the effect of specular and diffuse boundary surfaces is examined.

2. REM^2 for a plane-parallel system

2.1. Basic equations

We consider the participating medium in a plane-parallel system. The spectral radiation intensity I_ζ at r in the direction $\hat{s}$ can be expressed in terms of the radiation energy balance as follows:

$$\frac{\mathrm{d}I_\zeta(r,\hat{s})}{\mathrm{d}S} = -(\kappa+\sigma_s)I_\zeta(r,\hat{s}) + \kappa I_{b,\zeta}(T) + \frac{\sigma_s}{4\pi}\int_{4\pi} I_\zeta(r,\hat{s}')\phi(\hat{s}'\to\hat{s})\,\mathrm{d}\omega \quad (1)$$

where κ and σ_s are the spectral absorption and scattering coefficients, respectively. S is the path length in the direction $\hat{s}$. $\phi(\hat{s}'\to\hat{s})$ is the phase function from the direction $\hat{s}'$ to $\hat{s}$.

Equation (1) for a plane-parallel system with circumferential symmetry, as shown in Fig. 1, can be rewritten as

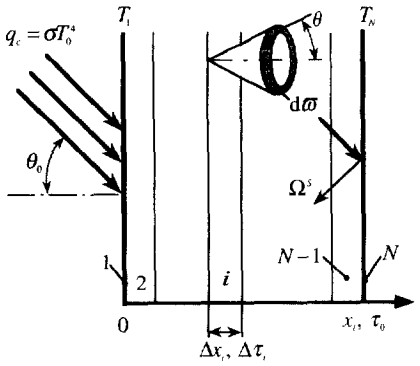

Fig. 1. Analysis model of plane-parallel medium.

$$\frac{dI_\lambda(x,\mu)}{dS} = \beta\left[-I_0(x,\mu)+(1-\Omega)I_{b,\lambda}(T) + \frac{\Omega}{2}\int_{-1}^{1} I_\lambda(x,\mu')\phi(\mu')\,d\mu'\right] \quad (2)$$

where β and Ω are the spectral extinction coefficient and the scattering albedo of the medium, respectively. μ is the direction cosine, $\mu \equiv \cos\theta$, and μ' is defined as $\mu' \equiv \hat{s}' \cdot \hat{s}$.

Considering the ith participating radiation element, we assume that each radiation element is at a constant uniform temperature T_i, and its refractive index n and heat generation rate per unit volume $q_{Xr,i}$ are also constant and uniform throughout the element. A ray passing through the radiation element attenuates by absorption and part of the ray is scattered. The ray is separated into absorbed, scattered and transmitted fractions. Moreover, it is assumed that the scattered radiation is distributed uniformly over the element.

As has been discussed by the author [8], the original REM^2 requires that radiation scattered and emitted from the participating media be isotropic. For anisotropic scattering media, we introduce an apparent extinction coefficient β^*, and thus, a corrected scattering albedo Ω^* by introducing the delta function approximation [14]. Details of the approximation and its validity are discussed in the following section. With this approximation, an anisotropic scattering medium can be treated as an isotropic scattering one. The third term on the right hand side of equation (2) is approximated [8] as

$$\frac{\Omega}{2}\int_{-1}^{1} I_\lambda(x,\mu')\phi(\mu')\,d\mu' \approx \frac{\Omega^*}{2}\int_{-1}^{1} I_\lambda(x,\mu')\,d^* \approx \Omega\mu' I_\lambda^D(x) \quad (3)$$

where $I_\lambda^D(x)$ is the average diffuse radiant intensity, i.e., the sum of the emitted and scattered radiant intensities [8]. Existing methods for analyzing radiation transfer in a plane-parallel system treat the participating medium and the boundary surfaces in separated ways. However, the author has pointed out that the relationship between the transmitted and diffusely scattered rays is the same as that between specular and diffuse reflections [6, 15]. In order to generally describe the boundary surfaces and participating media, the diffuse reflectivity of the surfaces and the corrected albedo of the participating media in equation (3) are redefined as Ω^D. The specular reflectivity Ω^S is also introduced to describe the specular reflectivity of the boundary surfaces.

A radiation element i can be regarded as either a volume element or a surface boundary. Equation (2) is integrated along the path length $S = \Delta x_i/\mu$ without taking into account incident radiation. Then the radiant energy emitted from the radiation element in the direction μ is given by

$$dQ_{J,i,\lambda(\mu)} = \mu[(1-\Omega_i^D-\Omega_i^S)I_{b,i,\lambda} + \Omega_i^D I_{i,\lambda}^D][1-\exp(-\beta^*\Delta x_i/\mu)]\,d\mu. \quad (4)$$

The parameters in equation (4) are given in Table 1 for various radiation elements. Integrating equation (4) over all discretized solid angles, the spectral radiation energy from the radiation element i, is given by

$$Q_{J,i,\lambda} = [(1-\Omega_i^D-\Omega_i^S)I_{b,i,\lambda}+\Omega_i^D I_{i,\lambda}^D] \times \sum_{k=1}^{K}\mu_k[1-\exp(-\beta^*\Delta x_i/\mu_k)]w_k \quad (5)$$

where μ_k, w_k and K are the discretized direction, the weight and the total number of discretized directions, respectively.

If $\beta^*\Delta x_i \gg 1$, the radiation element represents opaque solid. In the proposed radiation element method, both the surface and volume elements are accounted for by introducing the generalized form of radiation energy equations (4) and (5). Thus it is not necessary to distinguish between different types of elements. The effective radiation area A_i^R [16] is introduced as follows:

$$A_i^R \equiv \frac{1}{\pi}\int_{-1}^{1}\mu[1-\exp(-\beta^*\Delta x_i/\mu)]\,d\mu \approx \sum_{k=1}^{K}\mu_k[1-\exp(-\beta^*\Delta x_i/\mu_k)]w_k. \quad (6)$$

Finally, the rate at which radiation energy is emitted and isotropically scattered by the radiation element can be expressed in a generalized form as

$$Q_{J,i,\lambda} = \pi(\varepsilon_i I_{b,i,\lambda}+\Omega_i^D I_{i,\lambda}^D)A_i^R \quad (7)$$

where $\varepsilon_i = 1-\Omega_i^D-\Omega_i^S$ and $Q_{J,i,\lambda}$ is the diffuse radiation transfer rate, which was introduced in previous reports [6, 15], for arbitrary diffuse and specular surfaces.

2.2. Delta function approximation for anisotropic scattering media

In this section, the delta function approximation applied to the proposed method is briefly described. The

Table 1
Apparent extinction coefficients and albedos for various radiation elements

Radiation element	β^*	Ω^D	Ω^S
Isotropic medium	β	Ω	0
Anisotropic medium	$\beta(1-\Omega a_1/3)$	$\Omega(1-a_1/3)/(1-\Omega a_1/3)$	0
Surface boundary	$\beta^* S \gg 1$	Diffuse reflectivity	Specular reflectivity

phase function for an anisotropic medium is expanded in a series of Legendre polynomials as

$$\phi(\mu) = \sum_{n=0}^{\infty} a_n P_n(\mu) \tag{8}$$

where $P_n(\mu)$ is a Legendre function of order n, and a_n is the coefficient of the polynomial. Using the relationships in equations (9) and (10), a_0 is determined by equation (11):

$$\frac{1}{4\pi}\int_{4\pi} \phi(\theta)\,\mathrm{d}\omega = 1 \tag{9}$$

$$\int_{-1}^{1} P_n(\mu)\,\mathrm{d}\mu = 0 \quad (\text{for } n > 0) \tag{10}$$

$$\frac{1}{2}\int_{-1}^{1} \phi(\mu)\,\mathrm{d}\mu = \frac{1}{2}\int_{-1}^{1} \sum_{n=0}^{\infty} a_n P_n(\mu)\,\mathrm{d}\mu = a_0 = 1. \tag{11}$$

The phase function is approximated using $M+1$ terms of Legendre polynomials and the delta function as

$$\phi(\mu) \approx 2f\delta(1-\mu) + \sum_{n=0}^{M} A_n P_n(\mu) \tag{12}$$

where $\delta(1-\mu)$ and f are the delta function and the forward scattering fraction, respectively. The delta function is expanded in the following form [13]:

$$\delta(1-\mu) = \sum_{n=0}^{\infty} \frac{2n+1}{2} P_n(\mu). \tag{13}$$

The one-term approximation of equation (12), i.e. $M = 0$, represents isotropic scattering. Considering the relationship between equation (13) and the first two terms in equation (8), and comparing the coefficients with the one-term approximation of equation (12), then the anisotropic phase function is expressed in terms of the delta function approximation as

$$\phi(\mu) \approx 2f\delta(1-\mu) + A_0 = \frac{2}{3}a_1\delta(1-\mu) + \left(1 - \frac{a_1}{3}\right) \tag{14}$$

where a_1 is the coefficient of $P_1(\mu)$ in equation (8). In the above expression, only $(1-a_1/3)$ of the scattered rays are taken into account in the isotropic scattering. Since the absorbed fraction is not included in the scattering, the fraction of extinction in the medium does not change after the approximation in equation (14). Then the scaling corrections of β and Ω are required as discussed by Wiscombe [13].

Consequently the apparent extinction coefficient β^* and the corrected albedo Ω^D for the anisotropic medium can be expressed as

$$\beta^* = \beta[(1-\Omega) + \Omega(1-a_1/3)] = \beta(1-\Omega a_1/3) \tag{15}$$

$$\Omega^D = \frac{\beta\Omega(1-a_1/3)}{\beta^*} = \frac{\Omega(1-a_1/3)}{1-\Omega a_1/3} \tag{16}$$

β^* and Ω^D for various cases are listed in Table 1.

It should be noted that the apparent extinction coefficient is larger than the true extinction coefficient in the case of a strong back scattering medium or when $a_1 < 0$. The transmitted and diffuse scattered rays are separated in the ray tracing process in REM^2. The procedure based on the delta function approximation is the same as the ray tracing procedure in REM^2.

2.3. View factors

The author [6] has introduced absorption and diffuse scattering view factors for radiation transfer at diffuse and/or specular surfaces, in which specular reflection is not included [15]. Considering equation (4), we find that the rays isotropically scattered and transmitted through the radiation element can be treated in the same manner as those undergoing diffuse and specular reflection, respectively. Considering the radiation elements i and j, an extinction view factor $F^E_{i,j}$ is defined as the fraction of radiation energy leaving from radiation element i which is absorbed, isotropically scattered or diffusely reflected by radiation element j.

Using equation (5), $F^E_{i,j}$ can be written as

$$F^E_{i,j} = \sum_{k=1}^{K} f^j_i(\mu_k)\mu_k[1-\exp(-\beta^*_i\Delta x_i/\mu_k)] \times [1-\exp(-\beta^*_j\Delta x_j/\mu_k)]w_k \tag{17}$$

where $f^j_i(\mu_k)$ is the fraction of the energy emitted from element i in the direction μ_k which reaches element j. It is noted that $F^E_{i,j}$ for isotropic media can be applied to anisotropic media by introducing the scaling expressed in equations (15) and (16). As has been discussed in equations (4) and (5), the value $\beta^*_j\Delta x_j \gg 1$ for a boundary

surface element. For the surface elements, only the positive directions are considered, i.e. rays emitted towards the back face are not considered.

Surface elements and volume elements are treated separately for the calculation of view factors in the zone method [17]. It should be noted that surface and volume elements need not be treated separately in the proposed method by introducing equations (4) and (5). The above mentioned view factors, and generalized treatment can be achieved for both surface and volume elements.

There are several ways to choose the discrete directions μ_k and the weighting factors w_k. In the previous study [8] for complex 3-D configurations, the discrete directions were distributed uniformly over the solid sphere, or such that the weights of the discretized directions were uniform. In the present method, the discrete directions and weights are determined according to the discrete ordinates method [9] and are listed in Table 2. The ray emission at the boundary surface is conducted in a manner depending on the incident radiation as follows:

Diffuse irradiation:

Ray emission at surface boundary 1 is analyzed using the directions and weights in Table 2.

Collimated irradiation:

When the participating medium is exposed to a collimated irradiation flux, $q_c = \sigma T_0^4$, through boundary surface 1 with an incident angle θ_0, the parameters in equation (5) are set as

$$\mu_1 = \cos\theta_0, \quad w_1 = \pi, \quad K = 1, \quad \varepsilon_1 = 1. \tag{18}$$

It should be noted that the symmetric condition with respect to the axis, which is used for the diffuse boundary and participating media, is not applied for the case of collimated irradiation. Numerical ray tracing is carried out according to the method similar to the previous report [8].

Once the extinction view factors have been obtained,

Table 2
Discretized directions μ_k and their weights w_k for various numbers of discretization K [9]

K	μ_k	w_k
2	±0.5000000	6.2831853
4	±0.2958759	4.1887902
	±0.9082483	2.0943951
6	±0.1838670	2.7382012
	±0.6950514	2.9011752
	±0.9656013	0.6438068
8	±0.1422555	2.1637144
	±0.5773503	2.6406988
	±0.8040087	0.7938272
	±0.9795543	0.6849436

the absorption view factors $F^A_{i,j}$ and the diffuse scattering view factors $F^D_{i,j}$ can be written as [8]

$$F^A_{i,j} = \frac{\varepsilon_j F^E_{i,j}}{(1-\Omega^S_j)} \tag{19}$$

$$F^D_{i,j} = \frac{\Omega^D_j F^E_{i,j}}{(1-\Omega^S_j)}. \tag{20}$$

By introducing $F^A_{i,j}$ and $F^D_{i,j}$, the radiation transfer under arbitrary thermal conditions can be determined for each participating radiation element and boundary surface reported previously [8]. The proposed method can be used to solve the radiation transfer equation including specular boundary surfaces by introducing $F^A_{i,j}$ and $F^D_{i,j}$, as discussed in the next section.

2.4. Radiation transfer

The above-mentioned relations can be applied to the radiation transfer at each wave-length. However, in order to simplify the problem, the gray assumption is introduced in the following sections. Consider a system consisting of $N-2$ participating layers and two boundary surfaces, as shown in Fig. 1. We introduce the heat transfer rate of the irradiation energy, $Q_{G,i}$, and the emissive power $Q_{T,i}$ of the radiation element i:

$$Q_{G,i} = \sum_{j=1}^{N} F^E_{j,i} Q_{J,j} \tag{21}$$

$$Q_{T,i} = A^R_i \varepsilon_i n^2 \sigma T_i^4. \tag{22}$$

Considering the heat balance in an element and the diffuse radiation transfer rate per unit area $Q_{J,i}$ defined in equation (7), the net rate of heat generation $Q_{X,i}$ and $Q_{J,i}$ are derived as

$$Q_{X,i} = Q_{T,i} - \varepsilon_i Q_{G,i} \tag{23}$$

$$Q_{J,i} = Q_{T,i} + \Omega^D_i Q_{G,i} \tag{24}$$

where n is the refractive index of element i. Then, equations (23) and (24) can be rewritten as

$$Q_{X,i} = Q_{T,i} - \sum_{j=1}^{N} F^A_{j,i} Q_{J,j} \tag{25}$$

$$Q_{J,i} = Q_{T,i} + \sum_{j=1}^{N} F^D_{j,i} Q_{J,j}. \tag{26}$$

The heat transfer rate of the emissive power $Q_{T,i}$ or the net rate of heat generation $Q_{X,i}$ for each radiation element is given arbitrarily as a boundary condition. The unknown $Q_{X,i}$ or $Q_{T,i}$ can be obtained by solving equations (25) and (26) using the method described previously [6]. The relationships between T_i, $q_{X,i}$ and $Q_{T,i}$, $Q_{X,i}$ are obtained as

$$T_i^4 = \frac{Q_{T,i}}{A^R_i \varepsilon_i n^2 \sigma} \tag{27}$$

$$q_{X,i} = \frac{Q_{X,i}}{\Delta x_i} \tag{28}$$

where Δx_1 and Δx_N are unity in equation (28).

REM^2 can be applied to volume and surface elements in a similar manner, and the surface heat flux per unit surface area, $q_{X,s}$, and the volume heat generation rate per unit volume, $q_{X,v}$, are treated in the same manner as q_X. The radiation heat flux through the layer $q^R(x)$ is derived as

$$q^R(x) = q_{Xs,1} + \int_{x'=0}^{x} q_{Xv}(x')\,\mathrm{d}x'. \tag{29}$$

3. Results and discussion

3.1. Accuracy of analysis for isotropic scattering media

The proposed method, REM^2, is applied to plane-parallel and isotropic scattering media, and the results are compared with existing exact solutions.

We consider a participating medium of optical thickness τ_0. The medium is covered with isothermal black plates at temperatures T_1 and T_N. Since REM^2 can be used to analyze surface and volume elements in a similar manner, we specify radiation elements 1 and N as boundary surfaces and the other elements i $(i = 2 \ldots N-1)$ as volume elements with optical thickness $\Delta\tau \equiv \beta\Delta x$, as shown in Fig. 1.

First, we consider the case in which the medium does not generate heat i.e. $q_{Xv} = 0$, and the temperatures at the boundary surfaces are $T_1 = T_0$, $T_N = 0$. The dimensionless heat flux, given by equation (30), is calculated and compared with the exact solutions obtained by Heaslet and Warming [17]:

$$\Psi \equiv q^R/(\sigma T_0^4). \tag{30}$$

The deviation from the exact solution ΔE is defined as

$$\Delta E = \Psi/\Psi_{\text{exact}} - 1. \tag{31}$$

The effects of $\Delta\tau$ and the partition number N on the dimensionless heat flux are shown in Fig. 2. The variation of ΔE is expressed with a parameter $\Delta\tau$ or N. The number of discrete directions K in equation (5) is set at eight. The deviation, ΔE, increases as the thickness of the volume element $\Delta\tau$ increases. The accuracy of Ψ is strongly dependent on $\Delta\tau$. The deviation from the exact solution is less than 1% if the partition number N is chosen to be $\Delta\tau < 0.2$. The present results show good agreement with the analytical solutions. Since the participating medium does not generate heat and is at radiative equilibrium, the solution is independent of the albedo of the medium [19].

The effect of the discrete direction number K defined in equation (5) and given in Table 2 is examined in Fig. 3. In order to investigate the effect of K, the number of elements is fixed at $N = 102$. The accuracy of the proposed method is improved as the number of discrete directions increases. The deviation from the exact solution is less than 1% if $K \geqslant 6$. If we allow a 16% error in the estimation of the heat flux, then even $K = 2$ is useful. This rough approximation requires only one positive and one negative direction, and the calculation process then becomes very simple.

As an example of an isothermal medium, a non scattering participating medium is considered, i.e. $\Omega = 0$, $T_i = T_0$ $(i = 2 \ldots N-1)$, $T_1 = T_N = 0$. The dimensionless heat flux on the black surfaces is simply given [19] by

$$\Psi(0) = \Psi(\tau_0) = 2E_3(\tau_0) - 1 \tag{32}$$

where $E_3(\tau_0)$ is an exponential integral function of the third order.

The solution for an isothermal medium without scattering is independent of the partition number of the medium. Hence only one volume element is considered in the calculation in Fig. 4. An accurate solution can be obtained with $K \geqslant 6$ except in the case of very small optical thickness as shown in Fig. 4.

In summary for isotropic scattering media, the proposed method gives very accurate solution with small numbers of radiation elements and discrete directions. In particular, the method gives accurate results for inter-

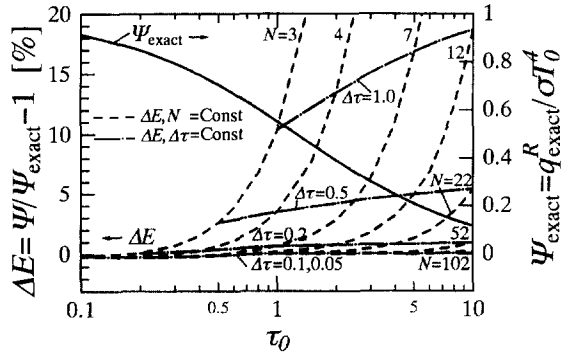

Fig. 2. Heat flux in adiabatic isotropic media, $q_{Xv} = 0$, $T_1 = T_0$, $T_N = 0$, $\phi(\mu) = 1$, $K = 8$.

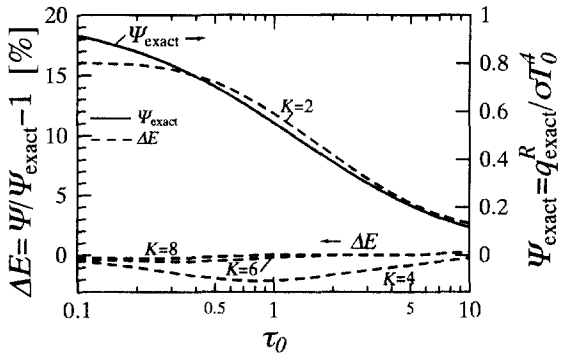

Fig. 3. Effect of number of discretized directions K on dimensionless heat flux, $q_{Xv} = 0$, $T_1 = T_0$, $T_N = 0$, $\phi(\mu) = 1$, $N = 102$.

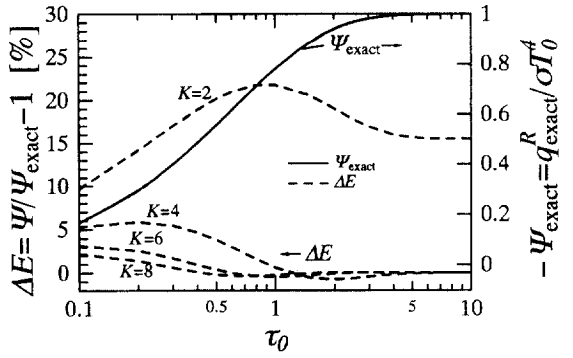

Fig. 4. Dimensionless heat flux in isothermal non-scattering participating media, $\Omega_i = 0$, $T_1 = T_0$, $T_1 = T_N = 0$.

mediate optical thickness for which neither the optically thin nor thick approximations can be applied.

3.2. Accuracy of delta function approximation for anisotropic scattering media

Anisotropic scattering media covered with isothermal black surfaces are considered in this section. In order to avoid needless uncertainty due to the numbers of elements and discrete directions, $N = 102$ and $K = 8$ are chosen in the following analysis.

As an example of simple anisotropic scattering media, the following linear anisotropic phase functions are considered:

$$\phi_0 = 1, \quad \phi_1(\mu) = 1 + 0.5\mu, \quad \phi_2(\mu) = 1 + \mu \tag{33}$$

where ϕ_0 is an isotropic phase function.

A pure scattering medium with $\Omega = 1$, $T_1 = T_0$, $T_N = 0$ is considered. The delta function approximation described in Section 2.2 is used to analyze the anisotropic medium. Participating media of various optical thicknesses are subjected to a diffuse or collimated irradiation flux from boundary surface 1. The reflectance $\rho^R = 1 - \Psi(0)$ is compared with the exact solutions obtained by Busbridge and Orchard [20].

The deviations from the exact solutions [20] for diffuse irradiation and normally collimated irradiation, i.e. $\theta_0 = 0$, are listed in Table 3. Very good accuracy is obtained for diffuse irradiation over the entire range of optical thickness. However, rather poor agreement is obtained for collimated irradiation and small optical thickness.

In order to examine anisotropic media with more complex phase functions, isothermal anisotropic media at $T_{r,i} = 0$ $(i = 2 \ldots N-1)$ is considered in Figs. 5 and 6. Strong forward scattering phase function ϕ_3 and back scattering phase function ϕ_4 are taken into account. The phase functions ϕ_3 and ϕ_4 are quoted from the ones by Lee and Buckius [11]. ϕ_3 and ϕ_4 are referred to as F2 and B1, respectively, in ref. [11]. These phase functions are plotted in Fig. 7.

When the temperatures at the boundary surfaces are set at $T_1 = T_0$, $T_N = 0$, the dimensionless transmitted flux τ^R and the reflected flux ρ^R of the layer can be expressed as

$$\tau^R = \Psi(x_l) \tag{34}$$

$$\rho^R = \cos\theta_0 - \Psi(0). \tag{35}$$

The results obtained using the present method are compared with the exact solutions obtained by Lee and Buckius [11] in Figs. 5 and 6. They are in very good agreement with each other. This indicates that not only strong forward scattering, as shown in Fig. 5, but also backward scattering media, as shown in Fig. 6, can be analyzed using REM^2 with the delta function approximation.

Most of the existing methods using delta function approximation adopt δ-Eddington approximation. The parameter M is set at 1 in δ-Eddington approximation, whereas M is set at 0 in the proposed method. The numerical treatment of the former becomes complicated as shown in an n-bounce method by Naraghi and Huan [17]. The numerical results obtained by REM^2 with much simpler approximation of anisotropic scattering shows good agreement with exact solutions.

From the above mentioned results, one can deduce that REM^2 can be applied to three-dimensional anisotropic media using the delta function approximation. If REM^2 can be used to analyze anisotropic media with complex configurations and thermal conditions, a variety of applications to both engineering and environmental problems can be expected.

3.3. Effect of specular boundary surfaces

We consider a participating medium composed of suspended glass particles of diameter $d_p = 10$ μm, and incident irradiation with a wavelength of $\lambda = 10$ μm. The wavelength is similar to that of a CO_2 laser. The real and imaginary parts of the complex refractive indices of the glass are 1.77 and 1.13, respectively [21].

The Mie scattering phase function $\phi(\mu)$ and the extinction and scattering coefficients of the particles are calculated using the method proposed by Bohren and Huffman [22]. The obtained phase function is shown in Fig. 7 as ϕ_5. The coefficient a_1 is obtained by

$$a_1 = \frac{3}{2}\int_{-1}^{1} \phi(\mu)\mu \, d\mu. \tag{36}$$

The calculated values of Ω and a_1 are 0.43 and 1.48, respectively.

For the boundary surface element N, vacuum plated pure nickel is examined. The normal reflectivity of the surface is 0.98 according to electromagnetic theory and the complex refractive index [23] for $\lambda = 10$ μm. There-

Table 3
Deviation from exact solutions for linear-anisotropic media, with $\Omega = 1$

$\phi(\mu)$	τ_0	Diffuse incidence ρ^R_{exact}	$\Delta E\%$	Collimated incidence ρ^R_{exact}	$\theta_0 = 0$ $\Delta E\%$
$\phi_0 = 1$	1	0.4466	−0.004	0.3413	0.074
	2	0.6099	−0.003	0.5175	−0.016
	5	0.7923	−0.007	0.7387	−0.017
	10	0.8833	−0.035	0.8530	−0.024
$\phi_1 = 1+0.5\mu$	1	0.4055	−0.209	0.2924	2.760
	2	0.5678	−0.055	0.4654	0.857
	5	0.7614	−0.013	0.6997	0.028
	10	0.8633	−0.023	0.8279	−0.023
$\phi_2 = 1+\mu$	1	0.3577	−0.607	0.2355	8.064
	2	0.5154	−0.158	0.4006	2.784
	5	0.7195	−0.003	0.6471	0.161
	10	0.8351	−0.014	0.7924	−0.014

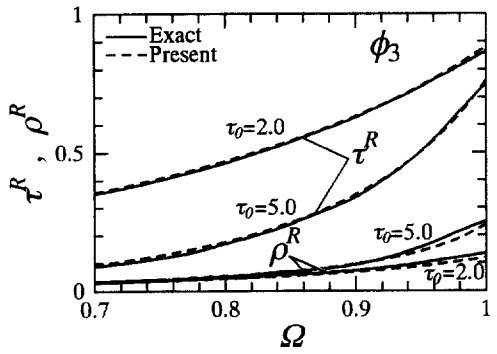

Fig. 5. Transmitted heat flux τ^R and reflected flux ρ^R of strongly forward scattering media, $\phi(\mu) = \phi_3$, $T_c = 0$, $T_1 = T_0$, $T_N = 0$.

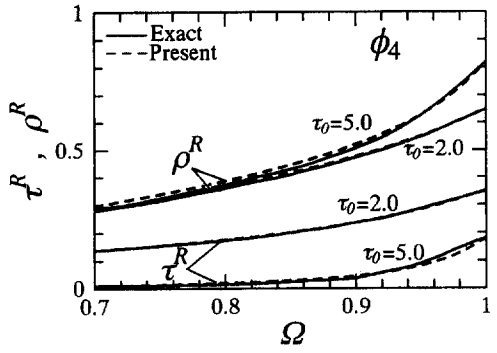

Fig. 6. Transmitted heat flux τ^R and reflected flux ρ^R of backward scattering media, $\phi(\mu) = \phi_3$, $T_c = 0$, $T_1 = T_0$, $T_N = 0$.

fore, we specify the specular reflectivity at the back boundary surface as $\Omega^S_N = 0.98$ or the diffuse reflectivity as $\Omega^D_N = 0.98$. $\varepsilon_1 = 1$ is specified for the other boundary surface 1.

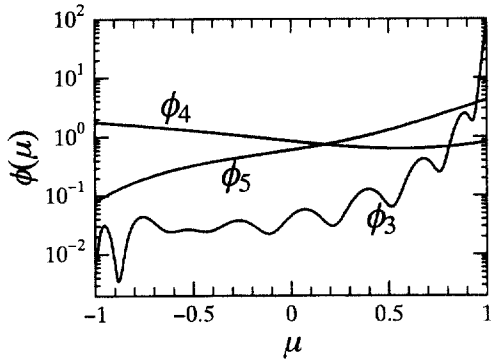

Fig. 7. Phase functions of various anisotropic media.

The participating medium is subjected to diffuse or collimated irradiation from boundary surface 1. When a collimated flux $q_c = \sigma T_0^4$ is irradiated at an incident angle θ_0, the heat flux from surface 1 is $q_c \cos\theta_0$. The heat flux is σT_0^4 for diffuse irradiation.

The transmitted flux for pure scattering isotropic media is calculated for various θ_0 using the present method, and compared with exact solutions [9]. The present results show very good agreement with the exact solutions.

The transmitted heat flux τ^R defined in equation (34) is examined for various conditions. Collimated irradiation flux at an incident angle $\theta_0 = 0$ or diffuse irradiation is applied on the participating media, and the results are shown in Fig. 8. Adiabatic ($q_{X_0} = 0$) or isothermal ($T_c = 0$) condition is considered. The transmitted flux for a specular back surface is smaller than that for a diffuse back surface when collimated incident flux is applied. This tendency is significant when the optical thickness is small and the layer is adiabatic. The difference is small

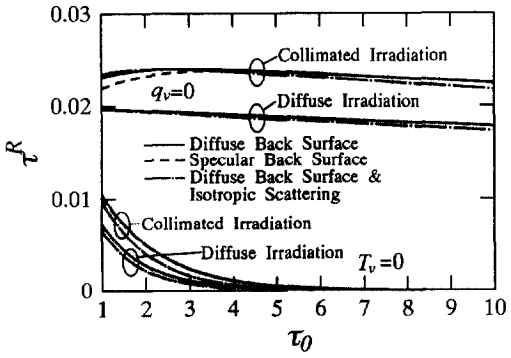

Fig. 8. Transmitted heat flux for various conditions. Collimated irradiation is normal to the surface.

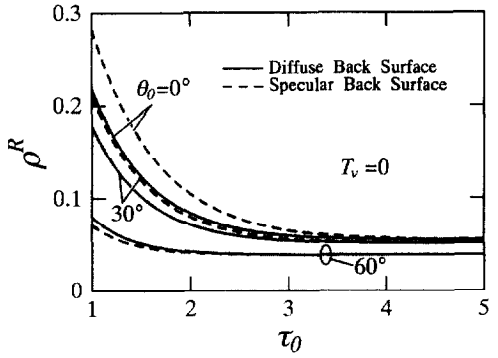

Fig. 10. Reflected flux of isothermal and anisotropic media against collimated incident irradiation.

for large optical thickness, diffuse irradiation and/or isothermal conditions. The transmitted flux for an isotropic medium is smaller than that for an anisotropic medium in most cases.

The effect of the incident angle of the collimated flux is examined in Fig. 9. Specular or diffuse back surface is examined. The thermal condition of the medium is adiabatic or isothermal. The transmitted flux is similar to that in Fig. 8. A specular back surface gives a smaller transmitted flux than a diffuse surface for small optical thickness, collimated irradiation and small θ_0. The transmitted fluxes for diffuse and specular boundaries are similar for the case of isothermal media.

The reflected flux ρ^R, given by equation (35) for isothermal media, is shown in Fig. 10. The value for adiabatic condition is expressed as $\rho^R = \cos\theta_0 - \tau^R$, since the radiation flux is constant throughout the layer. As shown in Fig. 10, the reflected flux for a specular back surface is larger than that for a diffuse surface for small optical thickness and collimated irradiation. The effect of the specular boundary diminishes if the optical thickness is larger than 4 under the present conditions. In the optically thick region, the reflected flux is constant, and independent of the optical thickness.

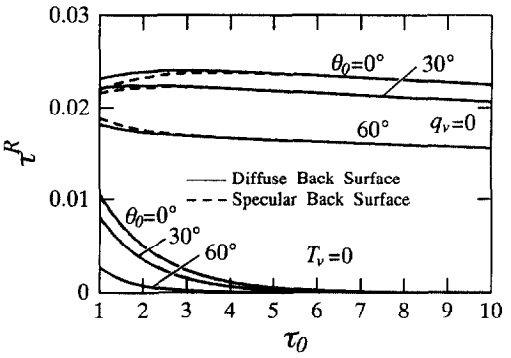

Fig. 9. Transmitted heat flux subjected to irradiation with various incident angles θ_0.

4. Conclusions

The radiation element method by ray emission model, REM^2, is applied to plane-parallel absorbing, emitting and scattering media with arbitrary thermal conditions in order to verify the applicability to anisotropic media. The surface boundary can be specular and/or diffuse with arbitrary thermal conditions. Diffuse or collimated irradiation can be applied at the boundary. The delta function approximation is adopted to scale the anisotropic scattering. REM^2 can be used to analyze a variety of thermal and boundary conditions, simply by changing the parameters of the radiation elements.

The accuracy of results obtained using REM^2 is confirmed by comparing them with existing solutions for isotropic scattering media. The proposed method gives very good accuracy for small numbers of radiation elements and discrete directions. The deviation from the exact solution is less than 1% when the optical thickness of the radiation elements is less than 0.2 and the number of discrete directions is larger than six. In particular, the method gives accurate results for intermediate optical thicknesses, for which neither the optically thin nor thick approximations can be applied.

REM^2 with the delta function approximation is applied to various anisotropic media, and the results obtained are compared with existing exact solutions. They show very good agreement, even for the cases of strong forward scattering and backward scattering media. Consequently, REM^2 can be applied to three-dimensional anisotropic media using the delta function approximation.

Radiation transfer for obliquely incident flux is analyzed, and the effects of specular and diffuse boundary surfaces are examined. The phase function of particles is

calculated using the Mie theory. The transmitted flux for a specular back surface is smaller than that for a diffuse surface when normally incident collimated flux is applied. This effect is significant when the optical thickness is small and the layer is adiabatic. The effect is small for large optical thickness, diffuse irradiation and/or isothermal conditions. The transmitted flux for isotropic media is smaller than that for anisotropic media in most cases.

Acknowledgement

The author would like to express his gratitude to Mr J. Yabana of the Institute of Fluid Science, Tohoku University, for his assistance in producing the graphs.

References

[1] Siegel R, Howell JR. Thermal Radiation Heat Transfer, 3rd ed. Washington DC: Hemisphere, 1992. pp. 795–804.
[2] Yang W-J, Taniguchi H, Kudo K. Radiative heat transfer by the Monte Carlo method. In: Hartnett JP, Irvine TF, editors. Advances in Heat Transfer. San Diego: Academic Press. 1995;27:3–211.
[3] Fiveland WA. Discrete ordinates solutions of the radiative transport equation for rectangular enclosures. ASME J Heat Transfer 1984;106:699–706.
[4] Lockwood FC, Shah NG. A new radiation solution method for incorporation in general combustion prediction procedures. Eighteenth International Symposium on Combustion. The Combustion Institute, 1981. pp. 1405–14.
[5] Bialecki RA. Solving heat radiation problems using the boundary element method. In: Brebbia CA, Connor JJ, editors. Topics in Engineering. Southampton, U.K.: Computational Mechanics Publications. 1993;15:67–89.
[6] Maruyama S. Radiation heat transfer between arbitrary three-dimensional bodies with specular and diffuse surfaces. Numerical Heat Transfer, Part A 1993;24:181–96.
[7] Maruyama S, Aihara T. Radiation heat transfer in absorbing, emitting and scattering media with arbitrary shapes and thermal conditions (basic theory and accuracy in plane-parallel system). Trans Japan Society of Mechanical Engineers 1994;60:3138–44.
[8] Maruyama S, Aihara T. Radiation heat transfer of arbitrary three-dimensional absorbing, emitting and scattering media and specular and diffuse surfaces. ASME J Heat Transfer 1997;119:129–36.
[9] Modest MF. Radiative Heat Transfer. New York: McGraw-Hill, 1993. pp. 541–85.
[10] Chai JC, Lee HS, Patankar SV. Ray effect and false scattering in the discrete ordinates method. Numerical Heat Transfer, Part B 1993;24:373–89.
[11] Lee H, Buckius RO. Scaling anisotropic scattering in radiation heat transfer for a planar medium. ASME J Heat Transfer 1982;104:68–75.
[12] Kim TK, Lee HS. Scaled isotropic results for two-dimensional anisotropic scattering media. ASME J Heat Transfer 1990;112:721–7.
[13] Wiscombe WJ. The delta-M method: Rapid yet accurate radiative flux calculations for strongly symmetric phase functions. J the Atmospheric Sciences 1977;34:1408–22.
[14] Crosbie AL, Davidson GW. Dirac-delta function approximations to the scattering phase function. J Quant Spectrosc Radiant Transfer 1985;33:391–409.
[15] Maruyama S, Aihara T. Radiation heat transfer of a Czochralski crystal growth furnace with arbitrary specular and diffuse surfaces. Int J Heat Mass Transfer 1994;37:1723–31.
[16] Maruyama S, Aihara T. Numerical analysis of radiative heat transfer from three-dimensional bodies of arbitrary configurations. JSME International Journal 1987;30:1982–7.
[17] Naraghi MHN, Huan J. An n-bounce method for analysis of radiative transfer in enclosures with anisotropically scattering media. ASME, J Heat Transfer 1991;113:774–7.
[18] Heaslet MA, Warming RF. Radiative transport and wall temperature slip in an absorbing planar medium. Int J Heat and Mass Transfer 1965;8:979–94.
[19] Ozisk MN. Radiative Transfer and Interactions with Conduction and Convection. New York: John Wiley and Sons, 1973. pp. 269–85.
[20] Busbridge IW, Orchard SE. Reflection and transmission of light by a thick atmosphere according to a phase function: $1+x\cos\theta$. The Astrophysical Journal 1967;149:655–64.
[21] Rubin M. Optical properties of soda lime silica glasses. Solar energy materials 1985;12:275–88.
[22] Bohren CF, Huffman DR. Absorption and Scattering of Light by Small Particles. New York: John Wiley and Sons, 1983. pp. 475–82.
[23] Lynch DW, Hunter WR. Comments on the optical constants of metals and an introduction to the data for several metals. In: Palik ED, editor. Handbook of Optical Constants of Solids. Orlando: Academic Press, 1985. pp. 313–23.